Parametrization of the Scattering Wave Functions of the Paris Potential

B. Loiseau[1] and L. Mathelitsch[2]

[1]Division de Physique Théorique*, Institut de Physique Nucléaire, F-91406 Orsay Cedex and LPTPE, Université Pierre et Marie Curie, 4 Place Jussieu 75252 Paris Cedex 05, France
[2]Institut für Theoretische Physik, Univ. Graz, Universitätsplatz 5, A-8010 Graz, Austria

ABSTRACT — The neutron-proton scattering wave functions of the Paris nucleon-nucleon potential are parametrized for partial waves of total angular momenta less than 5 ~~at laboratory kinetic energies between 0 MeV and 400 MeV~~. The inner parts of the wave functions are approximated by polynomials with a continuous transition to the outer parts, which are given by the asymptotic regime and determined by the respective phase shifts. ~~The smooth variation in energy of the phase shifts and of the coefficients of the polynomials permits~~ a ~~further parametrization of these quantities in terms of polynomials of low degree~~. The scattering wave functions can then be calculated at any given energy below 400 MeV. Special attention is devoted to the zero-energy limit of the low partial waves. An easy-to-use FORTRAN program, which allows the user to calculate these parametrized wave functions, is available via electronic mail.

IPNO/TH 96-41 OCTOBER 1996

* Unité de Recherche des Universités Paris 11 et Paris 6 Associée au CNRS

I — INTRODUCTION

Nucleon-nucleon (NN) scattering wave functions are important objects: they contain not only on-shell information like phase shifts, but also - as the t-matrix or the Noyes-Kowalski half-off-shell function - information about the off-shell behavior of the underlying NN interaction [1]. Furthermore, they play a crucial role in few-body problems, as the two-body input into these calculations is very often provided in terms of scattering wave functions. Examples for such applications are inelastic electron-deuteron scattering [2] or photodisintegration of the deuteron [3]. Moreover, the solution of nucleon-deuteron scattering via Faddeev-equations has become feasible in the last few years [4] and people are tackling already the exact solution of four- and more-body systems [5]. Furthermore the step from plane wave to distorted wave Born approximation (DWBA) requires the knowledge of scattering wave functions.

The calculation of the scattering wave functions is performed by solving the Schrödinger or, equivalently, the Lippman-Schwinger equation or some minimal-relativistic version of it, like the Blankenbecler-Sugar equation. The solution of these equations can be complicated, time consuming and tricky, for example in the very low-energy regime. These problems are even more severe when dealing with sophisticated realistic NN potentials like those of the Paris [6], Bonn [7] or Nijmegen [8] groups. In order to save time in applications, the Paris group has provided an easy-to-use parametrized form of the often needed bound state wave function of the deuteron [9]. This was followed by the Bonn group who parametrized deuteron wave functions of some of their potentials in exactly the same way [10]. However it is so far still necessary to solve the basic equation in order to get the scattering wave functions, and therefore rough approximations like the asymptotic forms of the wave functions or, even more crudely, plane waves are often used.

In this paper we will construct parametrizations of the scattering wave functions of the Paris potential in an energy range from zero energy up to a laboratory kinetic energy, T_L, of 400 MeV, and for total angular momenta, J, up to 4. Due to the explicit energy dependence of the scattering wave functions one has to parametrize - in principle - an

infinite set of functions. Making use of the smoothness of the energy-variation we will proceed in the following way. We will parametrize the inner part of the wave function, defined as the part where the actual wave function deviates from its asymptotic form, by a polynomial of a certain degree. The coefficients of the power series in the parameter r, the internuclear distance, are adjusted by a least square fit. The energy dependence of these coefficients is relatively weak and it is possible to parametrize them again by polynomials in the energy-variable.

The actual procedure has shown that the second part of this two-step process was not feasible over the entire energy range. Therefore we had to split this range into smaller regions, namely from $T_L = 0.1$ to 50 MeV, from 50 to 200 MeV and from 200 to 400 MeV. Since the wave functions with higher angular momentum ($L > 2$) are very small at low energies, the first interval of the fit for these waves is from 10 to 50 MeV with the other intervals as given above. The zero-energy waves need a different normalization than that usually applied. In order that the user can calculate wave functions at energies as small as wanted, we have parametrized the wave functions for $L < 3$ also with this new normalization from 0-5 MeV.

The number of partial waves to be taken into account is large, namely 14, and each partial wave is fitted within several regions. Therefore the output of the parametrization, necessary to calculate the requested wave functions, consists of large tables of parameters. It would not be of very practical use to publish these numbers. So, an easy-to-use FORTRAN program has been written and is available via electronic mail. It contains the sets of parameters and calculates the neutron-proton scattering wave functions together with the corresponding phase shifts. It allows for a simple and fast computation of the scattering wave functions for a given partial wave and energy and can also easily be implemented in other programs.

The present paper is organized as follows. Chapter II contains relevant formulae pertinent to scattering wave functions, including peculiarities at zero energy, details thereof are given in Appendix A. The procedure of the parametrization is described in Chapter III. The results are given in Chapter IV, and a description how to use the

FORTRAN program is also provided there. A table of numerical values of the fitted wave functions at $r = 1$ fm and at one energy in each interval of the fit is also given. It allows to check the proper use of the FORTRAN program. In order to check the accuracy of the fit we have calculated, in DWBA, matrix elements of the regularized one-pion-exchange potential with the original and the parametrized wave functions. Numerical results of this check are also given in Chapter IV. Details of the DWBA calculation are explained in Appendix B.

II — FORMALISM

The scattering wave function $\psi^k(r)$ of the relative motion of two nucleons is a solution of the Schrödinger equation

$$[T + V(\mathbf{r})]\psi^k(\mathbf{r}) = E\psi^k(\mathbf{r}). \tag{2.1}$$

T is the kinetic energy operator, E the center-of-mass relative energy related to the momentum k by

$$E = \frac{T_L}{2} = \frac{\hbar^2 k^2}{m}, \tag{2.2}$$

where m is the nucleon mass chosen here as the average neutron-proton mass, viz. 938.9190 MeV.

The peculiarity of the interaction enters via the potential $V(\mathbf{r})$. In the following we will use the NN potential which was derived by the Paris group. For the construction of the potential dispersion relations were applied including information from pion-nucleon and pion-pion scattering [11]. This ansatz gives a realistic description for the long and medium range of the interaction ($r > 1$ fm). For the short range part a phenomenological component was added, the parameters of which were adjusted by a fit to NN data up to a laboratory kinetic energy of $T_L = 330$ MeV. In order to facilitate applications, the energy dependence of the potential was cast into a velocity dependence, and the entire potential, theoretical and phenomenological part, was parametrized by a sum of Yukawa-type terms [6].

The Schrödinger equation was solved by the Paris group with a Runge-Kutta method integrating from small $r = 0.01$ fm to larger distances. The resulting wave functions were normalized by matching at $r = 15$ fm the numerical solution of the equation with the asymptotic waves and their first derivatives, expressions of which are given in Ref. 12. The velocity dependence of the potential was taken into account by a specific renormalization as explained in Ref. 13.

In the actual calculation one separates radial from angular and spin variables, and a decomposition into total, J, and orbital, L, angular momenta leads, for $\psi^k(\mathbf{r})$, to [14,15]

$$\begin{aligned}\psi^k(\mathbf{r}) = &\sum_{J=0}^{\infty} \frac{1}{r} u_J(k,r) Y_{J0}(\theta,\phi)\chi_{00} + \\ &+ \sum_{J=0}^{\infty} \sum_{L=J-1}^{J+1} \frac{1}{r} u_{JL}(k,r)\phi_{JML}(\theta,\varphi,\text{spin variables})\end{aligned} \tag{2.3}$$

with

$$\phi_{JML}(\theta,\varphi,\text{spin variables}) = \sum_{m=M-1}^{M+1} < LmSS_z \mid JM > Y_{Lm}(\theta,\varphi)\chi_{SS_z}. \tag{2.4}$$

Here, $u(k,r)$ denotes the radial part, χ_{SS_z} the spin function, $Y_{JM}(\theta,\varphi)$ the spherical harmonics, and the Clebsch-Gordan coefficient builds up the conserved total angular momentum J out of the orbital momentum L and spin S.

The first term in Eq. 2.3 belongs to the spin singlet, the second to the coupled and uncoupled triplet states. One can then rewrite $\psi^k(\mathbf{r})$ as

$$\psi^k(\mathbf{r}) = \sum_{J=0}^{\infty} [\psi^k_J(\mathbf{r}) + \psi^k_{JS_z\alpha}(\mathbf{r}) + \psi^k_{JS_z\beta}(\mathbf{r}) + \psi^k_{JS_z\gamma}(\mathbf{r})] \tag{2.5}$$

with, for the singlet wave,

$$\psi^k_J(\mathbf{r}) = \frac{u_J(k,r)}{r} Y_{J0}(\theta,\varphi)\chi_0 \tag{2.6}$$

for the uncoupled triplet wave,

$$\psi^k_{JS_z\gamma} = \frac{u_{JJ}(k,r)}{r}\phi_{JS_zJ} \tag{2.7}$$

and for the coupled triplet waves

$$\psi^k_{JS_z\alpha}(\mathbf{r}) = \frac{u_\alpha(k,r)}{r}\phi_{JS_zJ-1} + \frac{w_\alpha(k,r)}{r}\phi_{JS_zJ+1}$$
$$\psi^k_{JS_z\beta}(\mathbf{r}) = \frac{u_\beta(k,r)}{r}\phi_{JS_zJ-1} + \frac{w_\beta(k,r)}{r}\phi_{JS_zJ+1}. \tag{2.8}$$

The asymptotic forms of the radial parts can be expressed for the uncoupled waves by [12]

$$u^a_J(k,r) = cos\delta_J\ \hat{j}_J(kr) - sin\delta_J\ \hat{n}_J(kr) \tag{2.9}$$

and for the coupled ones by

$$\begin{aligned}
u^a_\alpha(k,r) &= -cos\epsilon_J[cos\delta_{J-1}\ \hat{j}_{J-1}(kr) - sin\delta_{J-1}\ \hat{n}_{J-1}(kr)],\\
w^a_\alpha(k,r) &= -sin\epsilon_J[cos\delta_{J-1}\ \hat{j}_{J-1}(kr) - sin\delta_{J-1}\ \hat{n}_{J-1}(kr)],\\
u^a_\beta(k,r) &= sin\epsilon_J[cos\delta_{J+1}\ \hat{j}_{J+1}(kr) - sin\delta_{J+1}\ \hat{n}_{J+1}(kr)],\\
w^a_\beta(k,r) &= -cos\epsilon_J[cos\delta_{J+1}\ \hat{j}_{J+1}(kr) - sin\delta_{J+1}\ \hat{n}_{J+1}(kr)].
\end{aligned} \tag{2.10}$$

$\hat{j}_J(kr)$ and $\hat{n}_J(kr)$ are the Riccati-Bessel and Riccati-Neumann functions related to the spherical Bessel functions of the first and second kind by $\hat{j}_J(kr) = kr\ j_J(kr)$ and $\hat{n} = kr\ n_J(kr)$. The phase parameters $\delta_{J\pm1}$, ϵ_J belong to the Blatt-Biedenharn parametrization [15].

In order that the zero-energy wave function is the limit as k goes to zero of the small-energy wave function, a slightly different normalization is useful (see Appendix A). The expression for the zero asymptotic energy uncoupled waves can be defined as

$$u^a_J(0,r) = \lim_{k\to 0}\frac{k^J}{sin\delta_J}u^a_J(k,r) = p_J\ r^{-J} - q_J\ \frac{r^{J+1}}{a_J} \tag{2.11}$$

with $p_0 = q_0 = 1$ and for $J > 0$

$$\begin{aligned}
p_J &= [1\cdot 3\cdot 5\cdots(2J-1)],\\
q_J &= [1\cdot 3\cdot 5\cdots(2J+1)]^{-1}.
\end{aligned} \tag{2.12}$$

Here, a_J is the scattering length of the J-wave. As explained in Appendix A the scattering length can be calculated without any ambiguity by solving the zero-energy Schrödinger equation.

The corresponding expressions to Eq. (2.11) for the zero-energy coupled case are

$$
\begin{aligned}
u^a_\alpha(0,r) &= -\lim_{k\to 0}\frac{k^{J-1}}{sin\delta_{J-1}}u^a_\alpha(k,r) = p_{J-1}\ r^{-J+1} - q_{J-1}\ \frac{r^J}{a_{J-1}},\\
w^a_\alpha(0,r) &= -\lim_{k\to 0}\frac{k^{J-1}}{sin\delta_{J-1}}w^a_\alpha(k,r) = \epsilon_{0J}\ p_{J+1}\ r^{-J-1},\\
u^a_\beta(0,r) &= -\lim_{k\to 0}\frac{k^{J+1}}{sin\delta_{J+1}}u^a_\beta(k,r) = \epsilon_{0J}\ q_{J-1}\ \frac{r^J}{a_{J+1}},\\
w^a_\beta(0,r) &= -\lim_{k\to 0}\frac{k^{J+1}}{sin\delta_{J+1}}w^a_\beta(k,r) = p_{J+1}\ r^{-J-1} - q_{J+1}\ \frac{r^{J+2}}{a_{J+1}}.
\end{aligned}
\tag{2.13}
$$

In these equations $a_{J\pm1}$ are the scattering lengths of the $J\pm1$ waves and ϵ_{0J} is specified by

$$
\epsilon_{0J} = \lim_{k\to 0}\frac{\epsilon_J(k)}{k^2}. \tag{2.14}
$$

III — PARAMETRIZATION

The radial parts $u_J(k,r)$, $u_{JJ}(k,r)$, $u_{\alpha,\beta}(k,r)$ and $w_{\alpha,\beta}(k,r)$ of the wave functions (see Eqs. 2.6 - 2.8) are parametrized in the following way. For a given energy (or equivalently for a given momentum k, see Eqs. 2.1 and 2.2) the full radial wave function $\tilde{u}_n(k,r)$ is split into its inner part ($r < r_{max}$) and its asymptotic part ($r \geq r_{max}$). Here the tilda denotes the parametrized wave and n corresponds to the orbital momentum: $n = J$ for $u_J(k,r)$ and $u_{JJ}(k,r)$, $n = J-1$ for $u_{\alpha,\beta}(k,r)$ and $n = J+1$ for $w_{\alpha,\beta}(k,r)$. The matching value r_{max} is chosen such that at this point the deviation between the value of the wave and of its asymptotic is already very small. r_{max} depends slightly on the angular momentum and more crucially on the energy. Its increase is of about 1 to 2 fm from lower to higher partial waves, as the stronger centrifugal barrier pushes the wave function to larger distances. On the other hand, the kinetic energy works against the barrier contribution, i.e. the higher the energy the more the wave function is pushed to smaller distances. For instance, for the P waves the asymptotic region starts around 5 to 6 fm for energies below $T_L \leq 10$ MeV and around 2 fm for $T_L > 300$ MeV.

Eqs. 2.9 and 2.10 are used for the asymptotic part, with the phase parameters δ_J, $\delta_{J\pm1}$, ϵ_J taken from the solution of the Schrödinger equation. For the inner part the numerical values of the wave functions are parametrized by a polynomial in r,

$$\tilde{u}_n(k,r) = \sum_{i=1}^{M} a_i^n(k) r^{n+i}. \tag{3.1}$$

The parameters $a_i^n(k)$ are adjusted by a least-square fit for $r_0 < r < r_{max}$. The parameter r_0 allows to cut off the very small-range region, where the waves are reproduced automatically by the constraint that $\lim_{r\to 0} u_n(k,r) = r^{n+1}$ and by the fit at higher r-values. For partial waves going to zero linearly in r ($^1S_0$ and $^3S_1 - ^3D_1$) we have insured the correct shape up to very small r values by performing an additional fit between 0 and 1 fm.

The least-square fit is further constrained to guarantee a smooth transition between the parametrized and the asymptotic regions, i.e.

$$\begin{aligned} \tilde{u}_n(k,r_{max}) &= \tilde{u}_n^a(k,r_{max}) \\ \tilde{u}_n'(k,r_{max}) &= \tilde{u}_n^{a'}(k,r_{max}), \end{aligned} \tag{3.2}$$

where the prime denotes the derivation with respect to r. The number of needed terms, M, varies from 7 to 10 - depending on the chosen partial wave and energy.

To get an analytic expression of the wave function over the entire energy range, one can, in a second step, parametrize the phase parameters δ_J, $\delta_{J\pm1}$ and ϵ_J, needed in the asymptotic part, and the parameters $a_i^n(k)$ of Eq. 3.1 for the inner part.

In the low energy range ($0 \le T_L \le 5$ MeV) the phase parameters δ_n are parametrized by an extension of the usual effective range expansion [16]

$$k^{2n+1} \cot \delta_n = -\frac{1}{a_n} + \frac{1}{2} r_n k^2 - P_n r_n^3 k^4 + Q_n r_n^5 k^6. \tag{3.3}$$

The scattering length a_n is known from the solution at zero energy of the Schrödinger equation, therefore just the parameters r_n, P_n and Q_n are fitted, again by a least-square procedure. The mixing parameter ϵ_J is fitted similarly by

$$\epsilon_J = \epsilon_{0J}\, k^2 + \sum_{j=1}^{3} c_j k^{2(j+1)}, \tag{3.4}$$

where ϵ_{0J} again is taken from the zero-energy solution of the Schrödinger equation. In the higher energy regions phases δ_n themselves are adjusted by the parameters c_j^n

$$\delta_n = \sum_{j=1}^{N} c_j^n k^{2j+1}. \tag{3.5}$$

In the average $N = 7$ or 8 terms give an excellent fit to the respective phases.

The parameters $a_i^n(k)$ are reproduced by the following expression

$$a_i^n(k) = b_{i0}^n + \sum_{j=1}^{N} b_{ij}^n (k - k_{min})^j, \tag{3.6}$$

where k_{min} corresponds to the lowest energy in each interval and $b_{i0}^n = a_i^n(k_{min})$. At the matching points of the intervals ($T_L = 50, 200$ MeV) it is more accurate to use the higher interval since the series (3.6) is expanded from the lowest point of the interval. The number of terms is in the average $N = 5$ to 8 to guarantee a good fit to $a_i^n(k)$.

The wave $\widetilde{u}_n(k,r)$ is now produced with the fitted values of $a_i^n(k)$, therefore Eqs. 3.2 do not hold anymore and a small discontinuity would exist in the wave functions at r_{max}. In order to guarantee a smooth behavior of the waves and their first derivatives, a cubic spline function connects the fitted and the asymptotic parts. Likewise a cubic function is introduced around 1 fm for the $^1S_0$ and the $^3S_1 - ^3D_1$ waves connecting fits done in the short and medium range parts.

IV — RESULTS

In the following we show and discuss the wave functions produced via the procedure described in the previous chapter. These wave functions can be obtained by a FORTRAN program available for users. We start with a short description how to get and how to use this program.

IV.1 The Program PARISWF

The program, which calculates the parametrized scattering wave functions of the Paris potential for partial waves up to $J \leq 4$ and for laboratory energies between $T_L = 0$ and 400 MeV, is written in double precision in FORTRAN 77. The main input, in particular the numbers of the coefficients c_j^n and b_{ij}^n of Eqs. 3.5 and 3.6, are given

in a BLOCK DATA subroutine. The actual size of the FORTRAN program, including a small main program calling PARISWF, is 342 blocks and 3142 FORTRAN lines on a VAX4000-90. The data need approximately 17000 units in double precision of array and the executable version of the program has a size of 291 blocks. The calculation of all waves at one energy and at 100 values of r, between 0 and 10 fm, takes less than 3 seconds of CPU time on a VAX4000-90.

The program is to be distributed via electronic mail and can be obtained from the authors. The corresponding e-mail addresses are LOISEAU@IPNCLS.IN2P3.FR and MATHELITSCH@KFUNIGRAZ.AC.AT. It can also be obtained via anonymous ftp from ftp.kfunigraz.ac.at, directory:/fbn/paris_ scatt_wf.

The user has to call a subroutine: PARISWF(TLAB, R, IWAV, IRENOR, TITWF, PHAS, WF, WFP). The program asks the user for the specification of 4 parameters of this list of arguments: the energy, the r value, the partial wave, and which normalization of the wave function should be used. The kinetic energy TLAB can be a real number between 0 and 400 and the real parameter R (internuclear distance r) should be larger than zero.The partial wave is indicated by an integer number IWAV ranging from 1 to 14 with the following correspondence to the individual quantum states: $^1S_0$ (IWAV = 1), $^3P_0$ (2), $^1P_1$ (3), $^3P_1$ (4), $^1D_2$ (5), $^3D_2$ (6), $^1F_3$ (7), $^3F_3$ (8), $^1G_4$ (9), $^3G_4$ (10), $^3S_1 - {}^3D_1$ (11),$^3P_2 - {}^3F_2$ (12), $^3D_3 - {}^3G_3$ (13), $^3F_4 - {}^3H_4$ (14). If a renormalization of the wave function is desired in order to provide the zero-energy calculation, the parameter IRENOR should be given a value of 1, otherwise IRENOR = 0. This different normalization (see Appendix A) is provided just for partial waves $J \leq 2$ and for energies between 0 and 5 MeV.

The output consists of the name of the partial wave, its phase, the values of the wave function and of its first derivative at the given energy and at the given internuclear distance. The corresponding parameters have to be declared as: CHARACTER*7 for TITWF and arrays for PHAS(3), WF(4) and WFP(4). TITWF gives the name of the partial wave asked by the user. For instance, if IWAV is 8, TITWF is $^3F_3$ and if IWAV=13, TITWF is $^3D_3 - {}^3G_3$. The rest of the output are double precision num-

bers: PHAS(1), WF(1) and WFP(1) are the phase, the value of the wave function and its derivative with respect to r for the uncoupled states. PHAS(1), PHAS(2) and PHAS(3) give the Blatt-Biedenharn parametrized values of δ_{J-1}, ϵ_J and δ_{J+1} coupled states. In this case, WF(i), for i=1 to 4, contain the values of $u_\alpha(k,r), w_\alpha(k,r), u_\beta(k,r)$ and $w_\beta(k,r)$, respectively. WFP(i), for i=1 to 4, contains their corresponding first derivatives. This simple call of the subroutine PARISWF(TLAB,R,IWAV,IRENOR, TITWF,WF,WFP) should allow for a fast and handy implementation in other programs.

In order to provide an easy test-run, a sample program PWF.FOR with a given input-data file PWF.DAT is mailed with the subroutine. The user is asked to test all partial waves she/he is going to use at each energy intervals needed. Correct values for all partial waves at a value of $r = 1$ fm and at one energy in each interval are given in the following subchapters to allow for a comparison with the user results.

IV.2 Zero energy expansion

As explained in Chapter II and in Appendix A the calculation of wave functions at zero energy requires a special renormalization of the wave function. Important quantities in this respect are the scattering lengths of the specific states. These scattering lengths were calculated from the solution of the Schrödinger equation at zero energy and they serve as input to the fit of the phases according to Eqs. 3.3 and 3.4. The parameters of the usual effective range expansion (Eq. 3.3) are given in Table 1 for uncoupled partial waves with $J \leq 2$. The corresponding results for the coupled states ${}^3S_1 - {}^3D_1$ and ${}^3P_2 - {}^3F_2$ are shown in Table 2, where expansion (3.3) is applied for the phases $\delta_{J\pm1}$ and equation (3.4) for the mixing parameter ϵ_J.

Though the zero-energy expansion is valid till 5 MeV in our program, we will show results just for zero energy. Fig. 1 gives the results for the isospin 1 uncoupled partial waves ${}^1S_0$, ${}^3P_0$, ${}^3P_1$, and ${}^1D_2$ respectively. Fig. 2 shows the results for the isospin 0 channels ${}^1P_1$, and ${}^3D_2$, again at $T_L = 0$ MeV. The precision of the approximation is so good that one barely sees a difference between the exact wave, indicated by symbols,

and the resulting one from PARISWF given by solid lines. Numerical values at $r = 1$ fm are given in Table 1 for the uncoupled partial waves, again at $T_L = 0$ MeV.

We have plotted in Figs. 3 and 4 the four waves $u_\alpha, w_\alpha, u_\beta, w_\beta$ as defined in Eq. 2.8 for the coupled states ${}^3S_1 - {}^3D_1$ and ${}^3P_2 - {}^3F_2$. Again the precision of the fit is rather good. The numerical values of the two triplet cases ${}^3S_1 - {}^3D_1$ and ${}^3P_2 - {}^3F_2$ at $r = 1$ fm and at zero energy are given in Table 3.

As explained in Appendix B one check of the quality of the fit consists in the comparison of the DWBA matrix elements of the regularized one-pion-exchange potential (Eqs. B6-B10). Table 4 gives as an example the values of the matrix elements for the calculation with the exact and the fitted wave functions for the ${}^1S_0$ and ${}^3S_1 - {}^3D_1$ cases. The agreement is better than 1%. This precision does not hold just for the waves exhibited in Table 4, but also similarly for all the other cases.

Another check consists in the calculation of the deviation between the exact and the approximated results by means of a χ^2 routine. We used the expression

$$\chi^2 = \frac{1}{N} \sum_{i=1}^{N} [u_n^{appr}(k, r_i) - u_n^{exact}(k, r_i)]^2 \tag{4.1}$$

with the number of mash points N being $N = 120$.

Again for illustration, we give in Table 5 the χ^2 values for one uncoupled (${}^1S_0$) and one coupled case (${}^3S_1 - {}^3D_1$). The quality of the fit with respect to χ^2 was very similar for all other cases.

IV.3 Scattering wave functions from 0.1 to 400 MeV

Phase shifts are important quantities in the construction of a scattering wave function since they determine entirely the asymptotic part (Eqs. 2.9 and 2.10). Therefore great emphasis was put on a good fit to the phases given by the Paris potential (Eqs. 3.3-3.5). Indeed the χ^2 per data point (the number of energies in a given interval is between 10 and 20) is better than $\chi^2 = 10^{-4}$ for the uncoupled phases. The quality of the fit is less good for the coupled waves, in particular the ${}^3H_4$ phase has a χ^2 of .015. The program

PARISWF can therefore be used also for the calculation of the phase shifts of the Paris potential to a very good accuracy.

As indicated above, the asymptotic wave is given with the same precision as the phase shift. The matching value r_{max} was finally adjusted such that the deviation of the asymptotic wave from the exact one was at r_{max} approximately the same as the difference between the fitted wave and the exact result, and, as already described above, a smoothing cubic function is inserted around r_{max}.

IV.3.1 Uncoupled partial waves

The isospin 1 uncoupled wave functions $^1S_0$, $^3P_0$, $^3P_1$ and $^1D_2$, are shown in Fig. 5, now for $T_L = 150$ MeV, and the isospin 0 states $^1P_1$ and $^3D_2$ in Fig. 2. Again the difference between the fitted and the exact waves can hardly be seen. The DWBA matrix elements are for the example of the $^1S_0$ wave $DWBA^{appr} = -.7469$ (compared to $DWBA^{exact} = -.7472$) for the energy of $T_L = 25$ MeV, $DWBA^{appr} = -.7247$ ($DWBA^{exact} = -.7263$) for 150 MeV, and $DWBA^{appr} = -.7205$ ($DWBA^{exact} = -.7351$) for 250 MeV, respectively. The χ^2 values for these cases are $\chi^2 = .59.10^{-4}, .88.10^{-4}$ and $.11.10^{-3}$.

In the average the quality of the fit decreases slightly in the high energy range in each interval. For the $^1S_0$ wave the worst case is at $T_L = 250$ MeV (the results are quoted above). The result of the parametrization of the other uncoupled waves is alike.

In order to allow a check of PARISWF we give in Table 6 values for all waves at $r = 1$ fm. The energies are chosen such that they lie more or less in the middle of each interval.

IV.3.2 Coupled partial waves

The important partial wave $^3S_1 - ^3D_1$ created the largest difficulty in the fit: to get a good result we had to split the 200-400 MeV energy range into two regions namely from 200 to 300 MeV and from 300 to 400 MeV. Therefore the check values of the waves

at $r = 1$ fm are also shown at four energies at $T_L = 25, 150, 250$ and 350 MeV (Table 7).

In general, the fit is not as good as for the uncoupled waves, in particular for the w_α and u_β waves, which represent the transition from $J \pm 1$ to $J \mp 1$. In Figs. 6 and 7 the results are plotted for $T_L = 150$ MeV for the cases ${}^3S_1 - {}^3D_1$ and ${}^3P_2 - {}^3F_2$. One difficulty with the coupled states was that the asymptotic wave gives a good approximation only at higher r values than for the uncoupled waves (r_{max} had to be as high as $r_{max} = 10$ fm in one case).

The accuracy of the DWBA matrix elements, with the example of the ${}^3S_1 - {}^3D_1$ wave at $T_L = 150$ MeV, are $DWBA^{appr} = -.5021$ ($DWBA^{exact} = -.4989$) for $I_{0,0}$, $DWBA^{appr} = 1.179$ ($DWBA^{exact} = 1.171$) for $I_{2,2}$, $DWBA^{appr} = 1.995$ ($DWBA^{exact} = 2.033$) for $I_{0,2}$. The χ^2 values for these waves are $1.2.10^{-5}$, $1.7.10^{-4}$, $1.9.10^{-5}$, and $9.8.10^{-6}$, respectively.

A similar accuracy is reached by all the other coupled waves. Fortunately, the not-so-good fit to the ${}^3H_4$ phase did not influence the wave function too much, because the phase has a small value compared to the phase of ${}^3F_4$ and to the mixing parameter ϵ_4. The DWBA value was good to .1% at 380 MeV and the χ^2 was $6.5.10^{-6}$.

The results of the remaining waves (${}^3P_2 - {}^3F_2, {}^3D_3 - {}^3G_3, {}^3F_4 - {}^3H_4$) are given in Table 8.

V — CONCLUSION

We have parametrized the phases and the scattering wave functions of the Paris potential from zero laboratory energy up to 400 MeV. The parametrization was done in a two-step process: First the scattering wave functions were approximated by a polynomial in r below a value of r_{max}, where the deviation of the scattering wave function from the asymptotic one is already very small. This was done for a variety of energies. Second, the coefficients of the first fitting procedure (as well as the scattering phases and the respective mixing parameters) were described by a polynomial in the energy (more

exactly in k^2). To achieve a good accuracy we had to split the entire energy range into 3 to 4 sections.

The quality of the approximation was tested by a χ^2 calculation and by using DWBA integrals with a regularized one pion exchange potential. Both tests showed a good to excellent quality of our results.

Scattering wave functions at very low energies are needed, e. g. for the calculation of atomic levels, and show some peculiarities. To allow for a smooth transition to the zero energy wave function, we parametrized the wave functions from 0 to 5 MeV laboratory energy in addition with a different normalization, as explained in the text and in Appendix A. We got a very satisfactory approximation to the exact wave functions also in this energy regime.

The main purpose of this work was that users should get access to the scattering wave functions of the Paris potential without having to solve the dynamic equation. In order to facilitate this supply we offer a computer program which includes the parametrization parameters and which calculates the parametrized wave functions for a given partial wave and at a given energy and r value. It can be implemented easily in other programs and should serve for more realistic calculations of nuclear processes.

Acknowledgements

We would like to express our gratitude for valuable comments and help to our colleagues G. Fäldt, M. Lacombe, W. Plessas, and C. Wilkin. The work was supported by the French-Austrian exchange program AMADEUS.

APPENDIX A

NORMALIZATION OF THE ZERO ENERGY NN WAVE FUNCTIONS

The zero-energy NN asymptotic partial wave functions, for coupled and uncoupled states, $u_n^a(0,r)$, satisfy the following reduced partial wave Schrödinger equation

$$u_n^{''a}(0,r) = \frac{n(n+1)}{r^2} u_n^a(0,r) \ . \tag{A.1}$$

The general solutions of this equation are

$$u_n^a(0,r) = \alpha r^{-n} + \beta r^{n+1} \ , \tag{A.2}$$

where α and β are constants determined by matching at large r ($r_a \simeq 15$ fm) the asymptotic waves and their first derivatives to the corresponding numerical solutions of the full Schrödinger equation. One obtains

$$\alpha = \frac{r_a^n}{(2n+1)}[(n+1)u_n(0,r_a) - r_a u_n^{'}(0,r_a)] \tag{A.3}$$

and

$$\beta = \frac{r_a^{-(n+1)}}{(2n+1)}[nu_n(0,r_a) + r_a u_n^{'}(0,r_a)] \ . \tag{A.4}$$

Here $u_n(0,r)$ and $u_n^{'}(0,r)$ are the numerical solutions and their first derivatives respectively. It is interesting to normalize the zero-energy solutions in such a way that they can be obtained as the limit, as the energy tends to zero, of the non-zero energy solutions.

The non-zero energy asymptotic partial waves, for uncoupled states, are usually chosen as in Eq. 2.9 and one can then define the zero-energy asymptotic solution according to Eqs. 2.11 and 2.12. The zero-energy uncoupled wave functions are then normalized as

$$u_J^N(0,r) = \frac{u_J(0,r)}{u_J(0,r_a)} u_J^a(0,r_a) \ . \tag{A.5}$$

Comparison of Eq. 2.11 with Eq. A.2 shows that the scattering length a_n which is defined as

$$a_n \equiv -\lim_{k\to 0}(k^{2n+1}\cot\delta_n)^{-1} \qquad (A.6)$$

is given by the ratio

$$a_n = -\frac{\alpha}{\beta}\,. \qquad (A.7)$$

This can be generalized to the coupled case and the asymptotic waves are given by Eqs. 2.13 and 2.14. Let us remark that the low energy expansion of Eq. B.13 of Ref. 12 shows that, at low energy, the nuclear bar phases, $\bar{\delta}_{J\pm1}$, of the Stapp parametrization [17], are equal to the corresponding Blatt-Biedenharn, $\delta_{J\pm1}$, phases. Furthermore for the nuclear bar coupling parameter, $\bar{\epsilon}_J(k)$ one has

$$\lim_{k\to 0}\frac{\bar{\epsilon}_J(k)}{k^{2J+1}} = -\epsilon_{0J}a_{J-1}\,. \qquad (A.8)$$

The normalization of the zero-energy coupled wave functions can then proceed in a similar way to that shown in Appendix B of Ref. 12 for non-zero energy waves. For completeness let us describe here the different steps which will also allow to give the expressions for the scattering lengths $a_{J\pm1}$ and the ϵ_{0J}.

One first builds up two independent sets of numerical solutions in such a way that their asymptotic limits behave like those of Eq. A.2. At large r one requires for the first set

$$\begin{cases} u_{J-1}(0,r)_{large\ r} = a_1 p_{J-1} r^{-J-1} + a_2 q_{J-1} r^{J} \\ w_{J+1}(0,r)_{large\ r} = b_1 p_{J+1} r^{-J+1} + b_2 q_{J+1} r^{J+2} \end{cases} \qquad (A.9a)$$

and for the second set

$$\begin{cases} \tilde{u}_{J-1}(0,r)_{large\ r} = \tilde{a}_1 p_{J-1} r^{-J-1} + \tilde{a}_2 q_{J-1} r^{J} \\ \tilde{w}_{J+1}(0,r)_{large\ r} = \tilde{b}_1 p_{J+1} r^{-J+1} + \tilde{b}_2 q_{J+1} r^{J+2}\,. \end{cases} \qquad (A.9b)$$

The coefficients, $a_i, b_i, \tilde{a}_i$ and $\tilde{b}_i$ $(i = 1,2)$ are obtained by equating at $r = r_a$ the numerical solutions of the two sets and their first derivatives to those of the asymptotic forms A.9a and A.9b. One obtains analogous expressions to those given in Eqs. A.3 and A.4. One can then define the following normalized sets

$$\begin{pmatrix} u^N_\alpha(0,r) \\ w^N_\alpha(0,r) \end{pmatrix} = \lambda \begin{pmatrix} u_{J-1}(0,r) \\ w_{J+1}(0,r) \end{pmatrix} + \mu \begin{pmatrix} \tilde{u}_{J-1}(0,r) \\ \tilde{w}_{J+1}(0,r) \end{pmatrix} \qquad (A.10a)$$

and

$$\begin{pmatrix} u_\beta^N(0,r) \\ w_\beta^N(0,r) \end{pmatrix} = \nu \begin{pmatrix} u_{J-1}(0,r) \\ w_{J+1}(0,r) \end{pmatrix} + \tau \begin{pmatrix} \tilde{u}_{J-1}(0,r) \\ \tilde{w}_{J+1}(0,r) \end{pmatrix} . \qquad (A.10b)$$

The λ, μ, ν and τ coefficients are determined by requiring the asymptotic limits of Eqs. A.9a and A.9b to be equal to the corresponding asymptotic waves given in Eq. 2.13. This leads to

$$\begin{aligned} \mu &= \frac{b_2}{b_2\tilde{a}_1 - a_1\tilde{b}_2} \\ \lambda &= -\mu\frac{\tilde{b}_2}{b_2} \\ a_{J-1} &= \frac{-1}{\lambda a_2 + \mu\tilde{a}_2} \\ \epsilon_{0J} &= \frac{b_2\tilde{b}_1 - b_1\tilde{b}_2}{b_2\tilde{a}_1 - a_1\tilde{b}_2} \end{aligned} \qquad (A.11a)$$

and

$$\begin{aligned} \tau &= \frac{a_1}{a_1\tilde{b}_1 - b_1\tilde{a}_1} \\ \nu &= -\tau\frac{\tilde{a}_1}{a_1} \\ a_{J+1} &= \frac{-1}{\nu b_2 + \tau\tilde{b}_2} \\ \epsilon_{0J} &= \frac{a_1\tilde{a}_2 - a_2\tilde{a}_1}{b_2\tilde{a}_1 - a_1\tilde{b}_2} . \end{aligned} \qquad (A.11b)$$

Constancy of the Wronskian,

$$\tilde{u}u' - u\tilde{u}' = w\tilde{w}' - \tilde{w}w' , \qquad (A.12)$$

which gives

$$a_1\tilde{a}_2 - a_2\tilde{a}_1 = b_2\tilde{b}_1 - b_1\tilde{b}_2 , \qquad (A.13)$$

shows that both expressions of ϵ_{0J} in Eqs. A.11a and A.11b are identical as it should be. The previous formulae can also be applied to scattering with an optical potential as in the antinucleon-nucleon process. In that case the waves, phases and zero-energy parameters are complex numbers.

Solving the zero-energy Schrödinger equation with the Paris potential [6] for neutron-proton scattering, i.e. for isospin T=0 and T=1 states, gives, for $J \leq 2$, the scattering lengths displayed in Table 1 for uncoupled waves and in Table 2, together with the ϵ_{0J} parameters, for coupled waves.

APPENDIX B

REGULARIZED ONE-PION EXCHANGE POTENTIAL DWBA INTEGRALS

In order to test the accuracy of our parametrized wave functions we shall compare integrals on r calculated with the exact Paris potential waves and with the parametrized ones. We consider integrals entering in the derivation of the partial-wave DWBA scattering amplitude. In the triplet-singlet basis the DWBA scattering matrix is

$$T_{\alpha\alpha'}^{DWBA} = e^{i(\alpha'-\alpha)\phi} < \psi_{\alpha'}^{k_f}(r)|V(r)|\psi_{\alpha}^{k_i}(r) > \qquad (B.1)$$

where α and α' denote the different total spin projections. For the transition potential we choose the one-pion exchange potential, regularized in the following way. One has, leaving out the isospin dependance $\tau_1 \cdot \tau_2$,

$$V(r) = V_\sigma(r)\sigma^1 \cdot \sigma^2 + V_T(r)S_{12}(\hat{r}) \qquad (B.2)$$

with the tensor operator

$$S_{12}(\hat{r}) = 3\sigma^1 \cdot \hat{r}\sigma^2\hat{r} - \sigma_1 \cdot \sigma_2 \qquad (B.3)$$

and

$$V_\sigma(r) = \frac{e^{-\mu r}}{r}(1 - e^{-\Lambda r}), \qquad (B.4)$$

$$V_T(r) = \frac{e^{-\mu r}}{r}\left(1 + \frac{3}{\mu r} + \frac{3}{\mu^2 r^2}\right)(1 - e^{-\Lambda r})^3. \qquad (B.5)$$

Here μ is the pion mass ($\mu = 138.04$ MeV for the isospin 0 potential and $\mu = 134.97$ MeV for isospin 1) and the short range regularization parameter Λ is taken to be $\Lambda =$ 1 GeV.

The different important integrals entering in the calculation of the partial wave of the scattering matrix (B.1) are given below. For the singlet amplitudes one has

$$I_J(k) = -3\int_0^\infty dr\ V_\sigma(r)(u_J(k,r))^2 \qquad (B.6)$$

and for the uncoupled triplet

$$I_{JJ}(k) = \int_0^\infty dr(V_\sigma(r) + 2V_T(r))(u_{JJ}(k,r))^2. \qquad (B.7)$$

For the coupled triplet transitions one needs to calculate

$$I_{J-1,J-1}(k) = \int_0^\infty dr \left[V_\sigma(r) - \frac{2(J-1)}{2J+1}V_T\right](u_\alpha(k,r))^2, \qquad (B.8)$$

$$I_{J+1,J+1}(k) = \int_0^\infty dr \left[V_\sigma(r) - \frac{2(J+2)}{2J+1}V_T\right](w_\beta(k,r))^2 \qquad (B.9)$$

and

$$I_{J-1,J+1}(k) = \int_0^\infty dr \frac{6\sqrt{J(J+1}}{2J+1}V_T(r)u_\beta(k,r)w_\alpha(k,r). \qquad (B.10)$$

REFERENCES

[1] P. Noyes, Phys. Rev. Lett. **15**, 538 (1965); K.L. Kowalski, Phys. Rev. Lett. **15**, 798 (1965).

[2] H. Arenhövel, W. Leidemann, and E.L. Tomusiak, Phys. Rev. C **46**, 455 (1992); B. Mosconi and P. Ricci, Nucl. Phys. **A517**, 483 (1990).

[3] H. Arenhövel and M. Sanzone, Photodisintegration of the Deuteron, Few Body Syst. Suppl. **3**, Springer Verlag, Wien, New York, 1991.

[4] W. Glöckle, H. Witala and Th. Cornelius, Nucl. Phys. **A496**, 446 (1989).

[5] W. Glöckle, H. Kamada, Phys. Rev. Lett. **71**, 971 (1993).

[6] M. Lacombe, B. Loiseau, J.M. Richard, R. Vinh Mau, J. Coté, P. Pirés, and R. de Tourreil, Phys. Rev. C **21**, 861 (1980).

[7] J. Haidenbauer, K. Holinde, and M.B. Johnson, Phys. Rev. C **45**, 2055 (1992); R. Machleidt, Adv. Nucl. Phys. **19**, 189 (1989).

[8] V.G.J. Stokes, R.A.M. Klomp, C.P.F. Terheggen, and J.J. de Swart, Phys. Rev. C **49**, 2950 (1994).

[9] M. Lacombe, B. Loiseau, R. Vinh Mau, J. Coté, P. Pirés, and R. de Tourreil, Phys. Lett. **101B**, 139 (1981).

[10] R. Machleidt, K. Holinde and Ch. Elster, Phys. Rep. **149**, 1 (1987).

[11] W.N. Cottingham, M. Lacombe, B. Loiseau, J.M. Richard, and R. Vinh Mau, Phys. Rev. **D8**, 800 (1973).

[12] B. Loiseau, L. Mathelitsch, and W. Plessas, Nuovo Cim. **97A**, 77 (1987); B. Loiseau, L. Mathelitsch, W. Plessas, and K. Schwarz, Phys. Rev. C **32**, 2165 (1985).

[13] F. Pauss, L. Mathelitsch, J. Coté, M. Lacombe, B. Loiseau, and R. Vinh Mau, Nucl. Phys. **A365**, 392 (1981).

[14] L. Hulthen and M. Sugawara, Handbuch der Physik **39**, 1 (1957).

[15] J.M. Blatt and L.C. Biedenharn, Phys. Rev. **86**, 399 (1952); Rev . Mod. Phys. **24**, 258 (1952).

[16] L. Mathelitsch and B.J. VerWest, Phys. Rev. C **29**, 739 (1984).

[17] H.P. Stapp, T.J. Ypsilantis and N. Metropolis, Phys. Rev. **105**, 302 (1957).

FIGURE CAPTIONS

Fig. 1 Uncoupled, isospin 1 and $J \leq 2$ parametrized zero energy wave functions (solid lines) compared to the exact ones (symbols).

Fig. 2 Uncoupled, isospin 0 and $J \leq 2$ parametrized wave functions at zero energy and at 150 MeV (solid lines) compared to the exact ones (symbols).

Fig. 3 $^3S_1 - 3D_1$ zero-energy wave functions (solid lines) compared to the exact ones (symbols).

Fig. 4 $^3P_2 - ^3F_2$ zero-energy wave functions (solid lines) compared to the exact ones (symbols).

Fig. 5 As in Fig. 1 but at 150 MeV.

Fig. 6 As in Fig. 3 but at 150 MeV.

Fig. 7 As in Fig. 4 but at 150 MeV.

Fig. 1

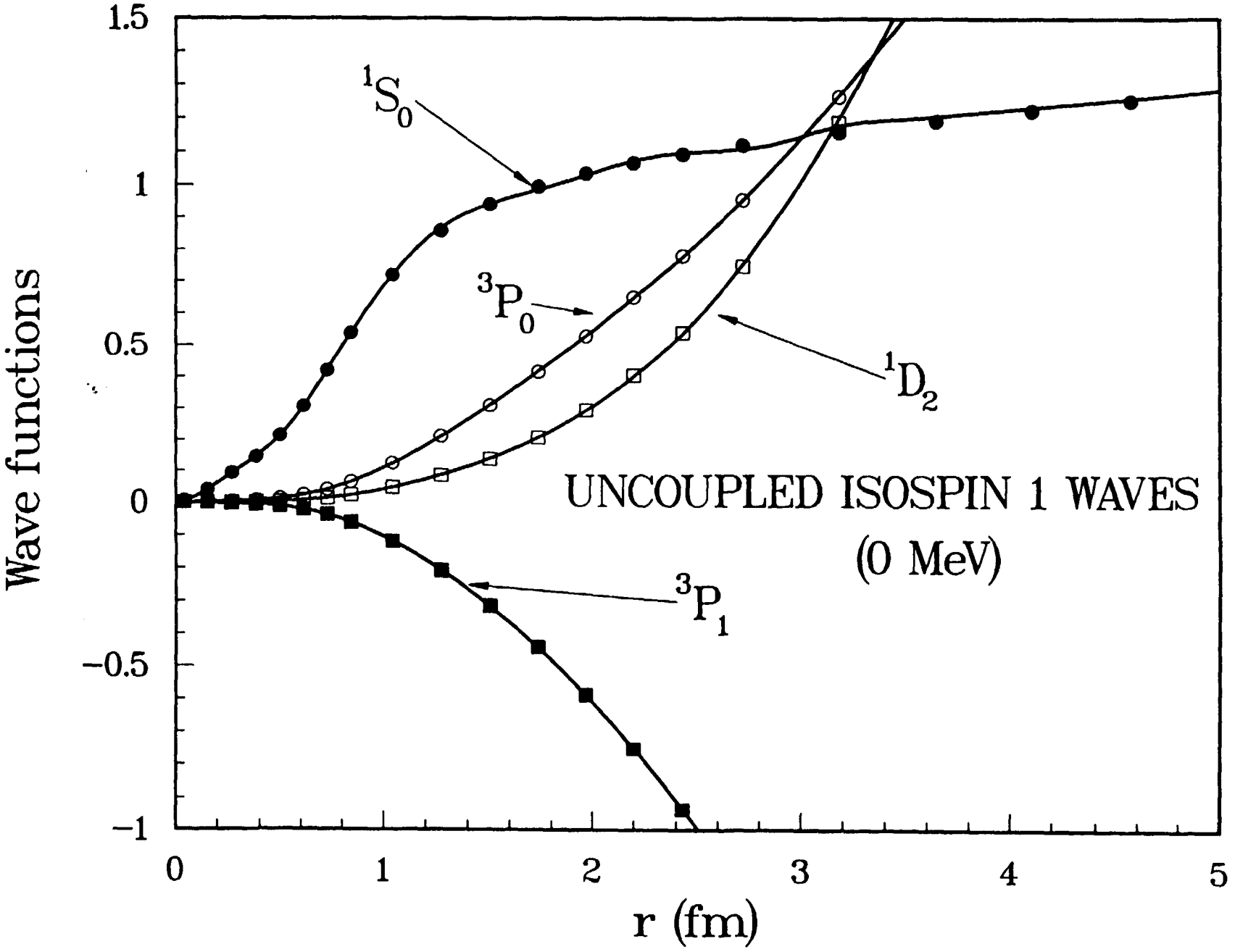
1.5
1
0.5
0
−0.5
−1
0
1
2
3
4
5
Wave functions
r (fm)
$^1S_0$
$^3P_0$
$^1D_2$
$^3P_1$
UNCOUPLED ISOSPIN 1 WAVES
(0 MeV)

Fig. 2

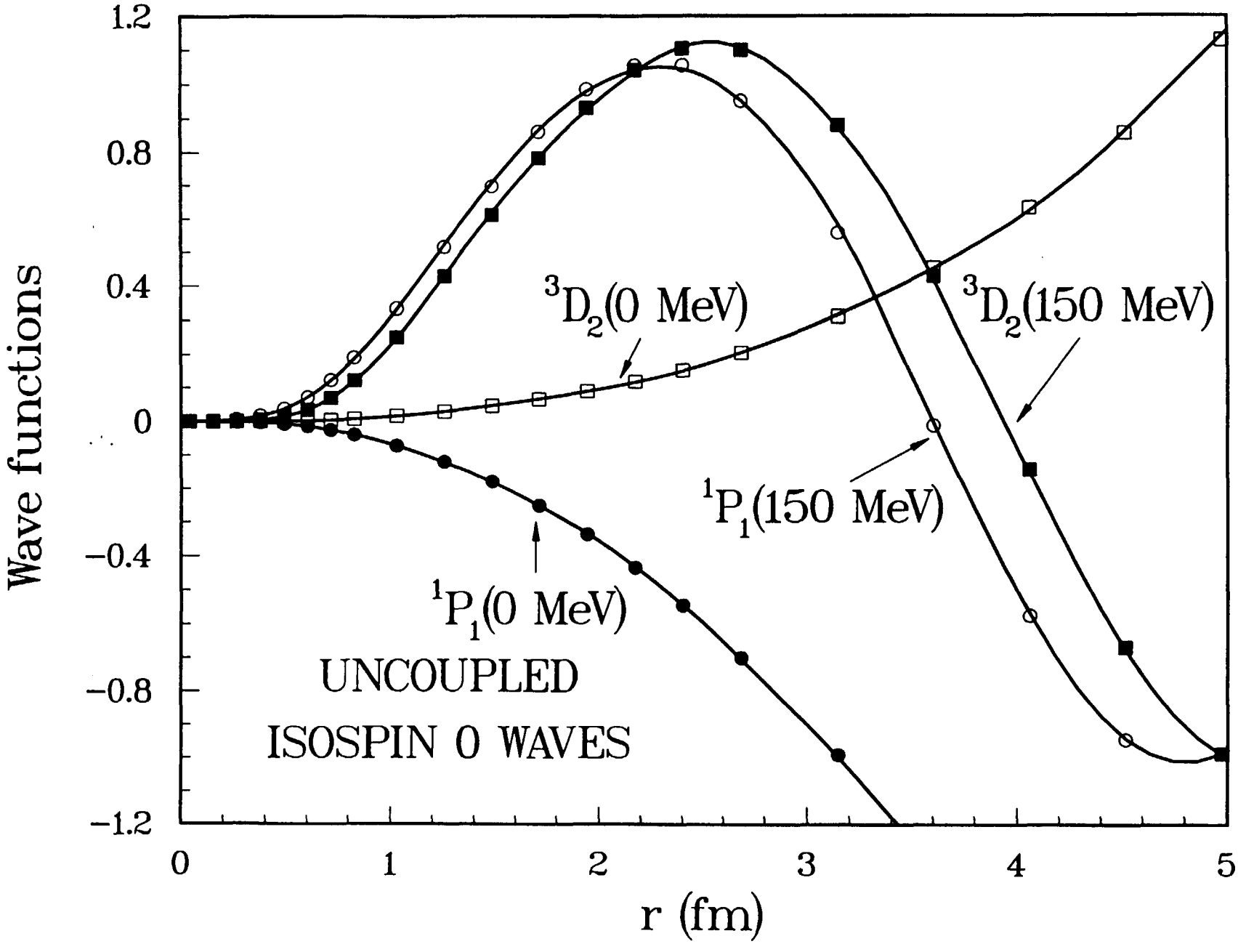
1.2
0.8
0.4
0
−0.4
−0.8
−1.2
Wave functions
0
1
2
3
4
5
r (fm)
$^3D_2$(0 MeV)
$^3D_2$(150 MeV)
$^1P_1$(150 MeV)
$^1P_1$(0 MeV)
UNCOUPLED
ISOSPIN 0 WAVES

Fig.3

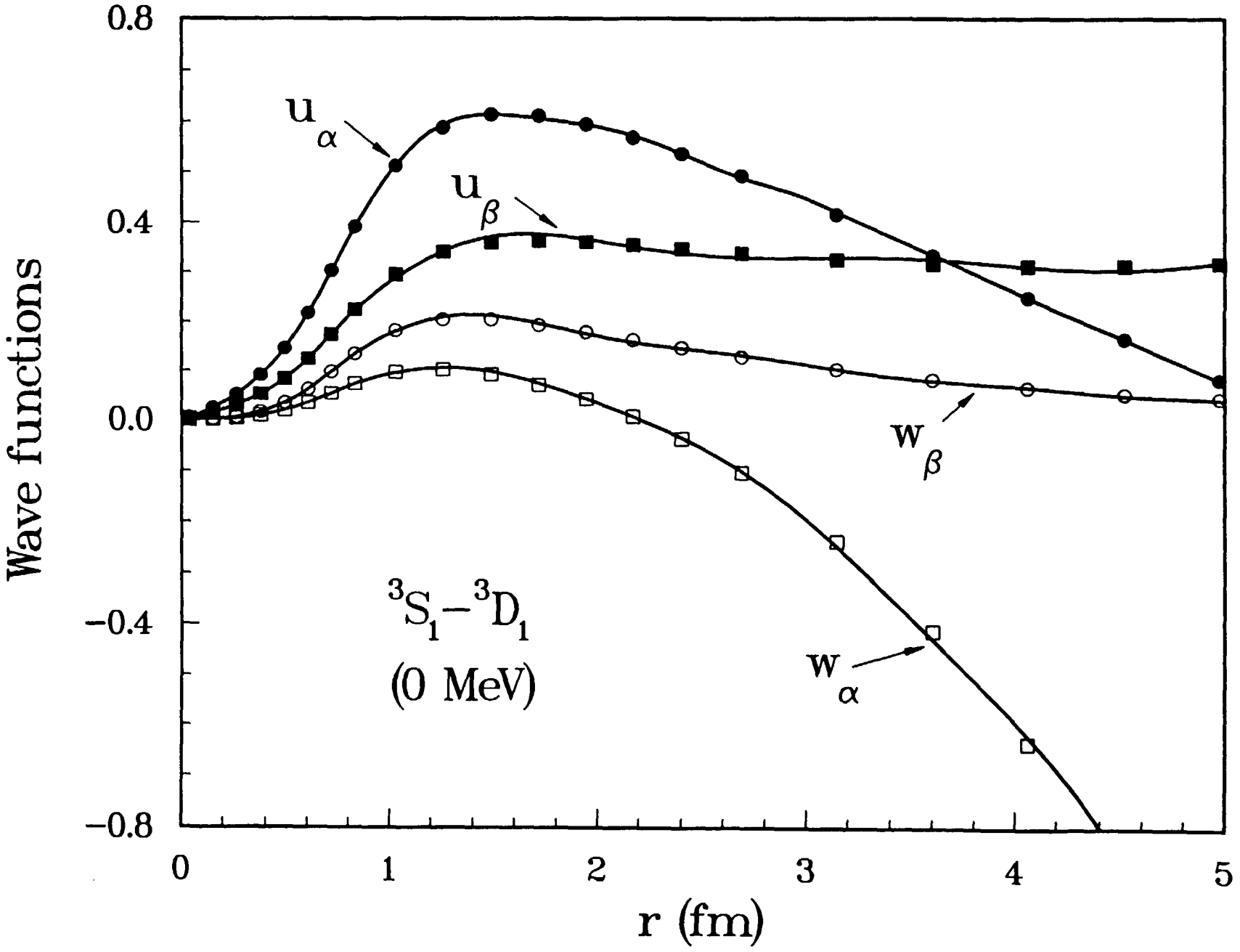
0.8
0.4
0.0
−0.4
−0.8
0
1
2
3
4
5
Wave functions
r (fm)
u_α
u_β
w_β
w_α
$^3S_1 - ^3D_1$
(0 MeV)

Fig. 4

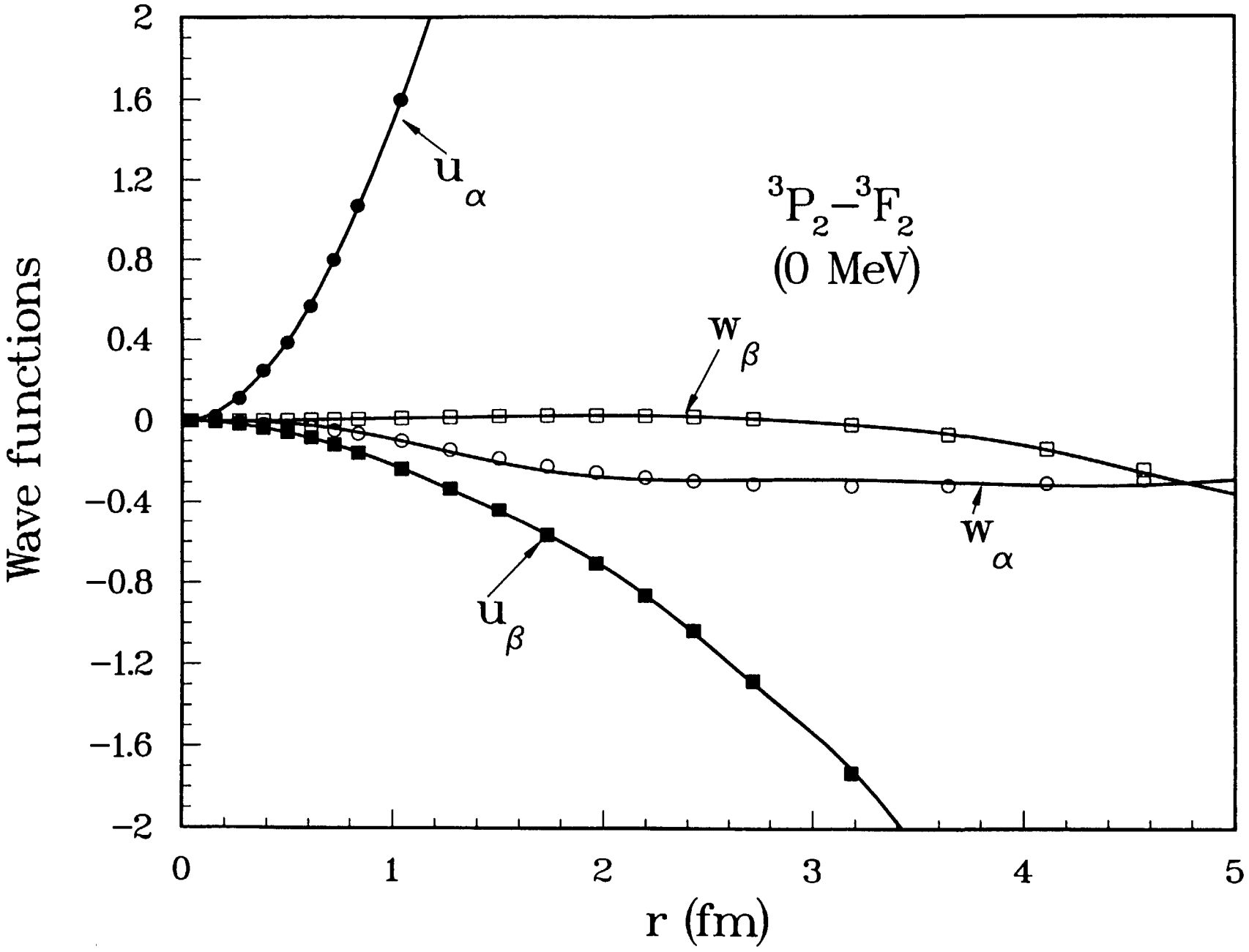
Wave functions
r (fm)
$^3P_2-^3F_2$
(0 MeV)
u_α
w_β
w_α
u_β
2
1.6
1.2
0.8
0.4
0
−0.4
−0.8
−1.2
−1.6
−2
0
1
2
3
4
5

Fig. 5

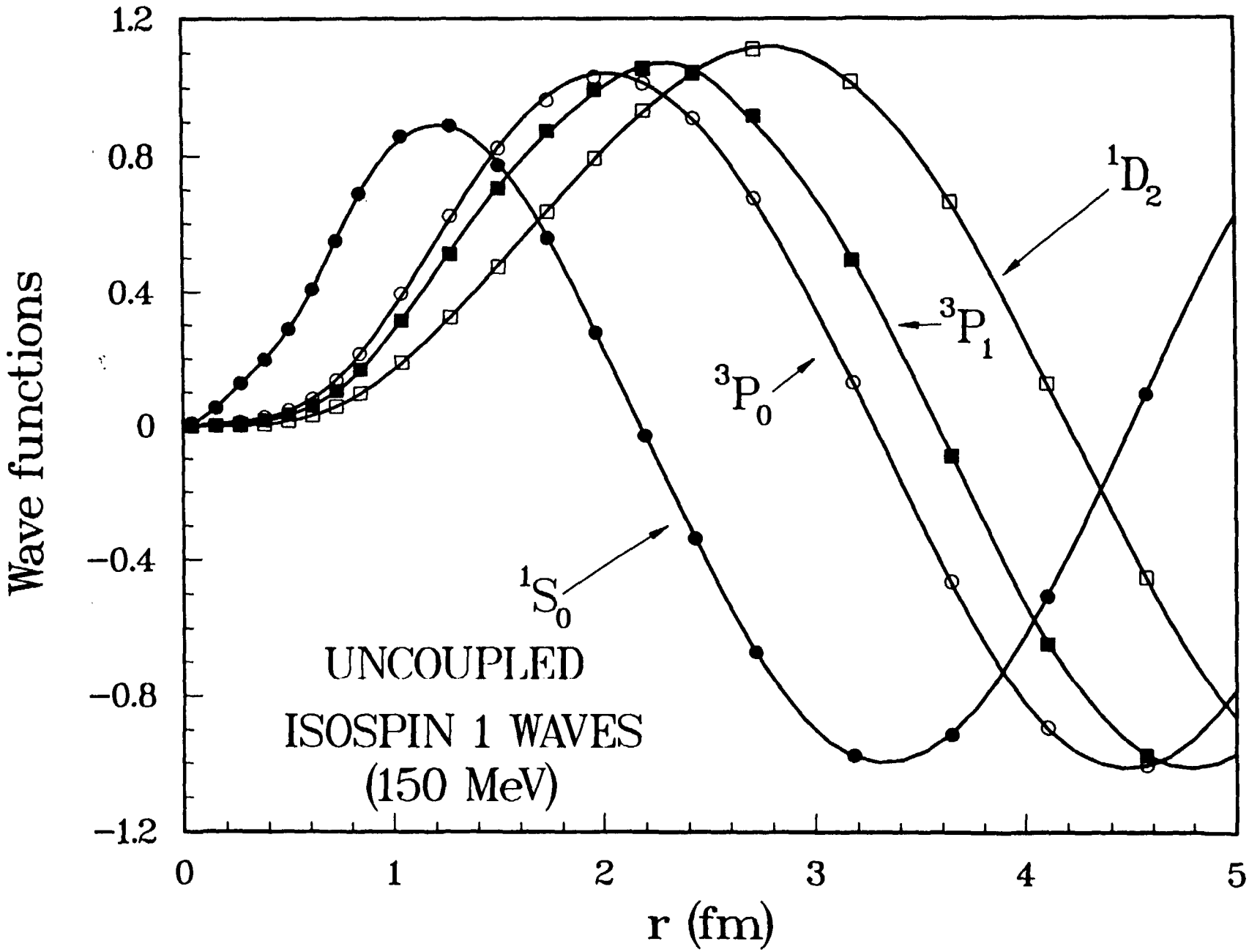
1.2
0.8
0.4
0
−0.4
−0.8
−1.2
Wave functions
0
1
2
3
4
5
r (fm)
$^1D_2$
$^3P_1$
$^3P_0$
$^1S_0$
UNCOUPLED
ISOSPIN 1 WAVES
(150 MeV)

Fig. 6

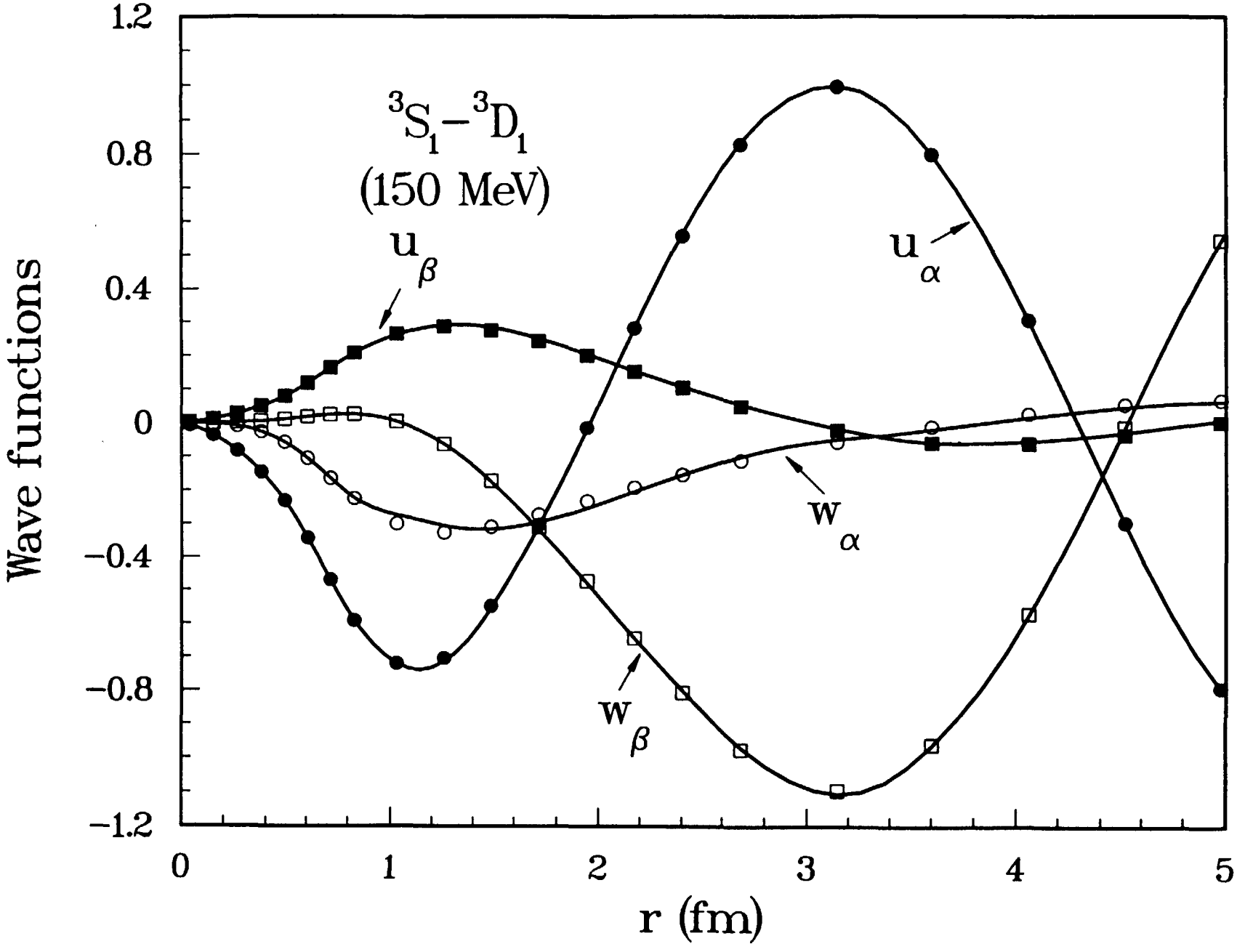
1.2
0.8
0.4
0
−0.4
−0.8
−1.2
0
1
2
3
4
5
Wave functions
r (fm)
$^3S_1 - ^3D_1$
(150 MeV)
u_β
u_α
w_α
w_β

Fig. 7

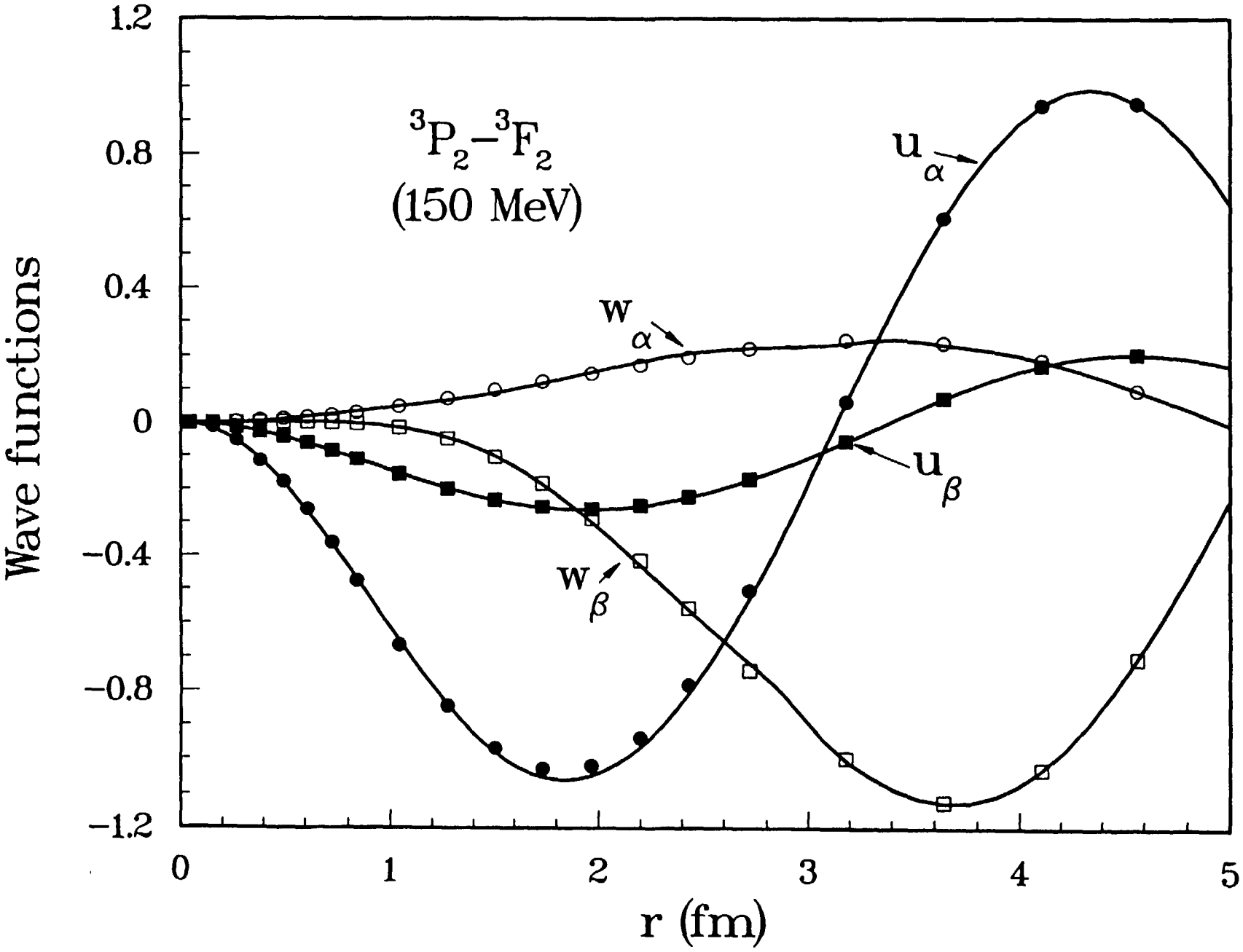
1.2
0.8
0.4
0
−0.4
−0.8
−1.2
0
1
2
3
4
5
Wave functions
r (fm)
$^3P_2$–$^3F_2$
(150 MeV)
u_α
w_α
u_β
w_β

$^{2S+1}L_J$	$^1S_0$	$^3P_0$	$^1P_1$	$^3P_1$	$^1D_2$	$^3D_2$
$a_n(\mathrm{fm}^{2l+1})$	$-.17618+02$	$.30445+01$	$.29663+01$	$.18488+01$	$-.18550+01$	$-.75656+01$
$r_n(\mathrm{fm}^{-2l+1})$	$.28830+01$	$.34855+01$	$-.57888+01$	$-.79767+01$	$.11419+02$	$.24558+01$
$P_n(\mathrm{fm}^{4l})$	$.29979-01$	$-.41965-01$	$-.14249-01$	$-.37844-02$	$-.13352-01$	$-.21293+00$
$Q_n(\mathrm{fm}^{4l})$	$.19383-01$	$-.39585-02$	$-.14232-02$	$-.30881-03$	$-.62149-04$	$-.34155-01$
$u(k=0,r=1\mathrm{fm})$	$.68693+00$	$.11031+00$	$-.66600-01$	$-.10413+00$	$.41608-01$	$.14384-01$

Table 1

Parameters of the effective range expansion and values of the zero-energy wave functions at $r = 1$ fm for uncoupled states.

	$^3S_1$	$^3D_1$	$^3P_2$	$^3F_2$	ε_1	ε_2	
$a_l(\mathrm{fm}^{2l+1})$	$.54273+01$	$.62578+01$	$-.29585+00$	$.14744+02$	$.17943+02$	$-.42334+02$	$\varepsilon_{0J}(\mathrm{deg.fm}^2)$
$r_l(\mathrm{fm}^{-2l+1})$	$.17658+01$	$-.31545+01$	$-.13268+02$	$-.32539+01$	$-.12393+03$	$.52725+04$	$c_1(\mathrm{deg.fm}^4)$
$P_l(\mathrm{fm}^{4l})$	$.61801-02$	$-.13692+00$	$-.14366-01$	$-.54818+00$	$.77344+03$	$-.33592+05$	$c_2(\mathrm{deg.fm}^6)$
$Q_l(\mathrm{fm}^{4l})$	$.96260-01$	$-.92034-02$	$-.20864-02$	$.21288+00$	$-.30712+04$	$.55836+05$	$c_3(\mathrm{deg.fm}^8)$

Table 2

Parameters of the effective range expansion (Eqs. (4.1) and (3.4)) for the coupled states $^3S_1 - {}^3D_1$ and $^3P_2 - {}^3F_2$.

	u_α	w_α	u_β	w_β
$^3S_1 - {}^3D_1$	.49845 + 00	.17587 + 00	.28111 + 00	.93752 − 01
$^3P_2 - {}^3F_2$	.14771 + 01	−.90206 − 01	−.21530 + 00	.13350 − 01

Table 3

Values of the zero-energy wave functions at $r = 1$ fm for the coupled states $^3S_1 - {}^3D_1$ and $^3P_2 - {}^3F_2$.

	$^1S_0$	$^3S_1 - {}^3D_1$		
	I_0	$I_{0,0}$	$I_{0,2}$	$I_{2,2}$
$DWBA^{exact}$	−0.961	−0.327	−1.56	0.676
$DWBA^{appr.}$	−0.966	−0.329	−1.57	0.676

Table 4

DWBA matrix elements as defined in Appendix B for the $^1S_0$ and $^3S_1 - {}^3D_1$ exact and parametrized wave functions at $T_L = 0$ MeV.

	$^1S_0$	$^3S_1 - {}^3D_1$			
	u_0	u_α	w_α	u_β	w_β
χ^2	.37 − 06	.49 − 07	.82 − 07	.65 − 06	.65 − 05

Table 5

χ^2 for the $^1S_0$ and $^3S_1 - {}^3D_1$ wave functions at $T_L = 0$ MeV.

T_L (MeV)	25	150	300
$^1S_0$	.70794 + 00	.82649 + 00	.85626 + 00
$^3P_0$	.96157 − 01	.34836 + 00	.52886 + 00
$^1P_1$	.54985 − 01	.30934 + 00	.56159 + 00
$^3P_1$	.53914 − 01	.28110 + 00	.46724 + 00
$^1D_2$	.12538 − 01	.16584 + 00	.37344 + 00
$^3D_2$	.19540 − 01	.22719 + 00	.43186 + 00
$^1F_3$	.59303 − 03	.19389 − 01	.69919 − 01
$^3F_3$	.66538 − 03	.22099 − 01	.78645 − 01
$^1G_4$	.54403 − 04	.45921 − 02	.23951 − 01
$^3G_4$	.56860 − 04	.49637 − 02	.25788 − 01

Table 6

Values of the wave functions of the uncoupled states at $r = 1$ fm at three different laboratory energies.

T_L(MeV)		25	150	250	350
$^3S_1 - {}^3D_1$	u_α	.59837 + 00	.70924 + 00	.69703 + 00	−.63394 + 00
	w_α	−.20627 + 00	−.27094 + 00	−.33020 + 00	−.39025 + 00
	u_β	.85621 − 01	.25621 + 00	.35962 + 00	.46945 + 00
	w_β	.23268 − 01	.92549 − 02	−.40144 − 01	−.87155 − 01

Table 7

Values of the wave functions of the $^3S_1$-$^3D_1$ coupled state at $r = 1$ fm at four different energies.

T_L(MeV)		25	150	300
$^3P_2 - {}^3F_2$	u_α	$-.12648+00$	$-.61620+00$	$-.87693+00$
	w_α	$.78450-02$	$.46045-01$	$.62930-01$
	u_β	$-.38487-01$	$-.14448+00$	$-.16489+00$
	w_β	$.20026-02$	$-.10220-01$	$-.57847-01$
$^3D_3 - {}^3G_3$	u_α	$-.74375-02$	$-.11697+00$	$-.27362+00$
	w_α	$-.15243-02$	$-.29283-01$	$-.78280-01$
	u_β	$.65678-02$	$.74595-01$	$.16525+00$
	w_β	$.12662-02$	$.13681-01$	$.22513-01$
$^3F_4 - {}^3H_4$	u_α	$-.75909-03$	$-.27933-01$	$-.10887+00$
	w_α	$.18281-04$	$.11919-02$	$.50802-02$
	u_β	$-.61033-03$	$-.17739-01$	$-.54136-01$
	w_β	$.94904-05$	$.30477-03$	$-.64833-03$

Table 8

Values of the wave functions of the three coupled states $^3P_2$-$^3F_2$, $^3D_3$-$^3G_3$, $^3F_4$-$^3H_4$ at $r = 1$ fm at three different laboratory energies.